Crumpling transition in tethered surfaces

Sherry Chu
Department of Physics, Massachusetts Institute of Technology
77 Massachusetts Avenue, Cambridge, MA 02139
(Dated: May 15, 2015)

We study the crumpling transition in tethered surfaces subject to different interactions, and provide numerical simulations for each case. Phantom tethered surfaces undergo a crumpling transition at finite bending rigidity κ_c. For $\kappa < \kappa_c$, the surface exhibits a crumpled phase, and the radius of gyration is $R_g \sim \sqrt{\ln L}$ where L describes the length of the surface; for $\kappa > \kappa_c$, the surface exhibits a flat phase, and $R_g \sim L$. Self-avoiding tethered surfaces, however, do not appear to exhibit a crumpled phase even at zero bending rigidity. We also investigate the effect of introducing a van der Waals attraction between neighbouring sites.

I. INTRODUCTION

The statistical mechanics of random surfaces and membranes in two dimensions has been studied extensively in the past [1][2]. The research has been motivated by wide-ranging applications in a number of different fields.

Fluctuating membranes are of great important in biological processes [3]. Much work has been done to study the properties of biological membranes, which can be considered as fluid, with negligible shear modulus. For example, a phospholipid molecule can diffuse freely across the cell membrane to adjust to the configuration of the membrane. Moreover, it is common for biological membranes to create or absorb vesicles through processes such as endocytosis, exocytosis, and budding, which introduces new geometrical considerations. Note that fluid membranes do not exhibit a finite temperature crumpling transition unless a long-range molecular interaction is introduced [4]. We will not discuss biological membranes further here, but instead focus on membranes with finite shear modulus.

In particular, we consider membranes with fixed connectivity. These crystalline or polymerized membranes describe systems where bonds between neighbouring sites cannot be broken. Such membranes exist in nature as cytoskeletons in cell membranes, and have also been realized in inorganic materials such as graphitic oxide (GO) [2]. Crystalline membranes are characterized by a bending rigidity κ and can undergo a finite temperature phase transition between a crumpled phase and a flat phase. The flat phase represents the breaking of a continuous symmetry, namely the orientation symmetry. However, this does not violate the Mermin-Wagner theorem, which states that there is no spontaneous breaking of continuous symmetry in two dimensions. The interactions between phonons lead to long-range interactions in the system [5]. More recently there has been interest in applying the theory of polymerized membranes to thermal excitations in graphene [6].

There exists also an intermediate configuration known as hexatic membranes, where the membrane is fluid but also has orientational order [7][8]. The equilibrium behaviour is then described by the bending rigidity κ and the hexatic stiffness K_A [7].

Although the topology of surfaces is much richer than that of polymers, and there is no single universality class which describes all random surfaces [2], we can nevertheless consider surfaces as a two-dimensional generalization of polymers. By characterizing surfaces with analogous definitions of the radius of gyration and persistence length, we can extract information about the critical behaviour of the surface near the crumpling transition.

II. TETHERED SURFACES

II.1. The model

The simplest model for surfaces with fixed connectivity is a tethered surface [9], where we consider each monomer to be tethered by a flexible string to its nearest neighbour sites. This corresponds to a nearest neighbour potential of the form

$$V_{nn}(r) = \begin{cases} \infty, & r > b, \\ 0, & r < b. \end{cases} \tag{1}$$

where r is the distance between nearest neighbours and b is the "bond length".

The specific structure of the underlying crystalline lattice or form of the tethering potential are, in fact, not important, as they do not affect the critical behaviour of the surface [10]. We will consider a triangular lattice with the above tethering potential for simplicity.

The nearest neighbour interaction energy is then

$$E_{nn} = \sum_{\langle \mathbf{x}, \mathbf{x}' \rangle} V_{nn}(|\mathbf{r}(\mathbf{x}) - \mathbf{r}(\mathbf{x}')|). \tag{2}$$

II.2. Flory Theory

Consider the tethered surface as a D-dimensional generalization of a polymer embedded in d-dimensional space, with $D = 2$ and $d = 3$. The Landan-Ginzburg free-energy must preserve translational and rotational symmetries, and takes the form [11]

$$\mathcal{F} = \int d^D x \left[\frac{t}{2} (\partial_\alpha \mathbf{r})^2 + u(\partial_\alpha \mathbf{r} \cdot \partial_\beta \mathbf{r})^2 \right. \tag{3}$$

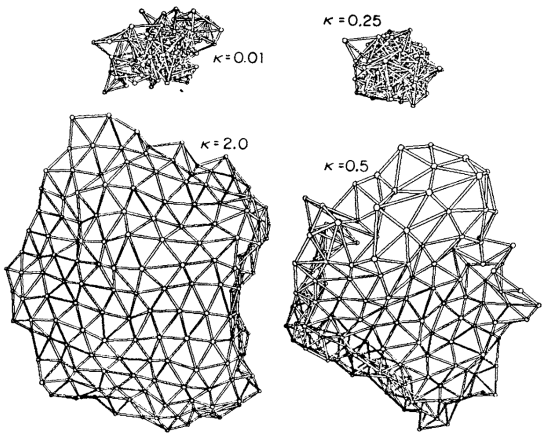

FIG. 1. Monte Carlo simulations for phantom tethered surfaces with different values of bending rigidity κ [10].

$$+v(\partial_\alpha \mathbf{r}\cdot\partial_\alpha \mathbf{r})^2+\frac{\kappa}{2}(\partial_\alpha^2\mathbf{r})^2+\cdots\Big]$$

where $\alpha,\beta\in\{1,\dots D\}$.

Scaling arguments give an estimate for the exponent ν_f in Flory theory [12] defined by $R\sim L^{\nu_f}$ as

$$\nu_f=\frac{D+2}{d+2}. \tag{4}$$

For self-avoiding two-dimensional surfaces embedded in three spatial dimensions, the Flory scaling exponent is $\nu_f=0.8$.

III. PHANTOM SURFACES

We begin by considering phantom surfaces, which are allowed to freely intersect with itself. We show using Monte Carlo simulations that such surfaces undergo a crumpling transition at finite bending rigidity κ_c.

III.1. Crumpled phase

For a phantom surface with zero bending rigidity, the only interaction is the nearest neighbour tethering potential. Monte Carlo simulations show that for a sufficiently low bending rigidity, the surface exhibits a crumpled phase at equilibrium (see Fig. 1).

III.1.1. Gaussian surface

The behaviour of the surface can be obtained analytically for a Gaussian interaction energy [9]

$$V(r)=\frac{K}{2}\left(\frac{r}{a}\right)^2. \tag{5}$$

where a is a short-distance cut-off on the order of the lattice spacing. Note that a potential of this form assumes interaction between sites through long chains, with energies proportional to the squared end-to-end distance. In general, we cannot prove that the potential for a tethered surface approaches this form [10].

The mean-squared separation is

$$\langle|\mathbf{r}(\mathbf{x})-\mathbf{r}(\mathbf{x}')|^2\rangle\simeq\frac{k_BTda^2}{\sqrt{3}\pi K}\ln\left(\frac{|\mathbf{x}-\mathbf{x}'|}{a}\right) \tag{6}$$

for $|\mathbf{r}(\mathbf{x})-\mathbf{r}(\mathbf{x}')|\gg a$. The radius of gyration squared is

$$R_G^2=\frac{1}{2A^2}\int d^2x d^2x'\langle|\mathbf{r}(\mathbf{x})-\mathbf{r}(\mathbf{x}')|^2\rangle \tag{7}$$

where A is the area of the surface. Thus for the Gaussian potential, the radius of gyration scales as $R_G\sim\sqrt{\ln L}$.

Furthermore, a Migdal-Kadanoff bond-moving approximation can be applied. Tethering potentials such as the rigid rod model or the flexible string model have been shown to converge numerically to a Gaussian potential, indicating that they belong to the same universality class [9].

III.2. Flat phase

A surface with high bending rigidity remains approximately flat, and we can parametrize the height fluctuations using the Monge representation, where the height is described as a function of position, $\mathbf{r}(\mathbf{x})=(x_1,x_2,h(x_1,x_2))$. The free energy of the surface [13] is then

$$\mathcal{F}=\int d^2x\left[\frac{\kappa}{2}(\nabla^2h)^2+\frac{1}{2}(2\mu u_{ij}^2+\lambda u_{kk}^2)\right] \tag{8}$$

where κ is the bending rigidity, μ and λ are the Lamé coefficients, and u_{ij} is the strain tensor defined as

$$u_{ij}=\frac{1}{2}(\partial_iu_j+\partial_ju_i+\partial_ih\partial_jh). \tag{9}$$

In constrast, in a fluid surface, the second term in the free energy vanishes, and the surface crumples [10].

In Monte Carlo simulations, the bending ridigity is commonly introduced explicitly by defining the bending energy [14]

$$E_b=\frac{\kappa}{2}\sum_{\langle\alpha\beta\rangle}|\mathbf{n}_\alpha-\mathbf{n}_\beta|^2=\kappa\sum_{\langle\alpha\beta\rangle}(1-\mathbf{n}_\alpha\cdot\mathbf{n}_\beta) \tag{10}$$

where $\mathbf{n}_\alpha$ is the surface normal associated with the triangular plaquette α. In Fig. 1, we see that for large enough κ, the surface exhibits a flat phase at equilibrium.

III.3. Crumpling transition

The equilibrium behaviour of fluid membranes and rigid membranes are qualitatively different, indicating the existence of a phase transition at finite bending rigidity κ_c. This transition can be quantified by performing

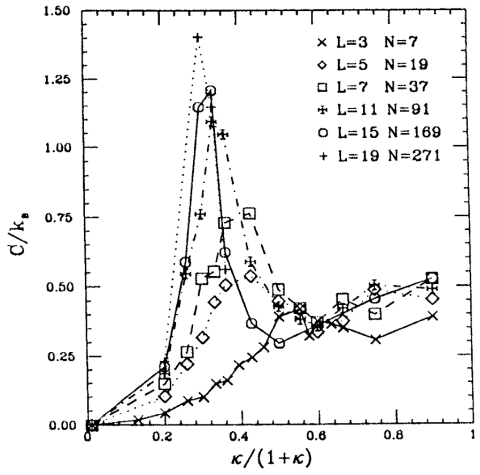

FIG. 2. Specific heat per monomer C as a function of bending rigidity κ for different values of L [14]. The heat capacity due to kinetic energy is not shown.

numerical simulations on the L-dependence of the radius of gyration R_g [10]. In the thermodynamic limit,

$$R_g(L) = \begin{cases} \xi\sqrt{\ln L}, & \kappa < \kappa_c, \\ \zeta L, & \kappa > \kappa_c, \end{cases} \tag{11}$$

where the parameters ξ and ζ depend on κ. Near the critical bending rigidity, there exists a transitional "semi-crumpled" phase with $R_g \sim L^{\nu'}$ where $\nu' \simeq 0.8$ [10].

Further evidence of the crumpling transition can be found by computing the specific heat per monomer C as a function of κ. The specific heat is obtained as [14]

$$C = \frac{k_B\kappa^2}{N}\left[\left\langle\left(\sum_{\langle\alpha,\beta\rangle}\mathbf{n}_\alpha\cdot\mathbf{n}_\beta\right)^2\right\rangle - \left\langle\sum_{\langle\alpha,\beta\rangle}\mathbf{n}_\alpha\cdot\mathbf{n}_\beta\right\rangle^2\right] \tag{12}$$

The dependence on κ is plotted in Fig. 2 for different values of L. The heat capacity due to kinetic energy is not shown. For $\kappa = 0$, we expect $C = 0$, since fluctuations are purely entropic, and the only contribution to the heat capacity arises from the kinetic energy. On the other hand, for $\kappa \to \infty$, we expect $C = k_BT/2$, since the transverse fluctuations are entropic, and do not contribute. We see that Fig. 2 is consistent with these predictions in the two limiting cases. The peak in the specific heat indicates a phase transition at $\kappa_c \simeq 0.5$. Moreover, the peak increases with system size L, suggesting that the phase transition is not first order.

IV. SELF-AVOIDING SURFACES

In this section we consider the effects of self-avoidance. In the flat phase, the self-avoiding constraint should be unimportant, since it is unlikely for an approximately flat surface to self-intersect. However, we expect the constraint to become relevant in the crumpled phase, and lead to swelling of the crumpled surface.

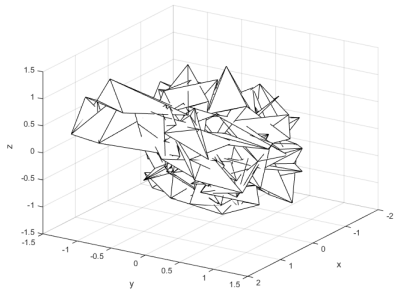

(a)Phantom surface with $L = 20$ and tethering interaction parameter $b = 1.2$.

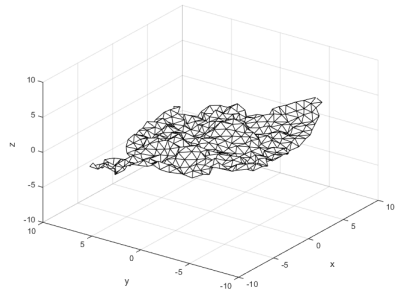

(b)Self-avoiding surface with $L = 20$, excluded volume parameter $a = 0.7$, and tethering interaction parameter $b = 1.2$.

FIG. 3. Monte Carlo simulations for phantom and self-avoiding tethered surfaces with zero bending rigidity.

As in the case of polymers, an analytic solution is no longer possible when we introduce self-avoidance effects. We rely instead on numerical simulations to provide insight into the equilibrium behaviour.

We introduce the self-avoiding constraint via a hard-sphere interaction between all sites on the surface.

$$V_{sa}(r) = \begin{cases} 0, & r > a, \\ \infty, & r < a. \end{cases} \tag{13}$$

The associated energy is then

$$E_{sa} = \frac{1}{2}\sum_{\mathbf{x},\mathbf{x}'} V_{sa}(|\mathbf{r}(\mathbf{x}) - \mathbf{r}(\mathbf{x}')|). \tag{14}$$

Note that this definition is more accurately described as an excluded volume interaction. For a triangular lattice, the surface is self-avoiding for $a > b/\sqrt{3}$. The self-avoiding constraint can also be defined more directly by forbidding each site from crossing any plaquette in the surface.

In Fig. 3, the results of Monte Carlo simulations for the self-avoiding tethered surface at zero bending rigidity are compared to those for a phantom surface under the same simulation conditions. The equilibruim behaviour of the self-avoiding surface clearly differs from that of the phantom surface.

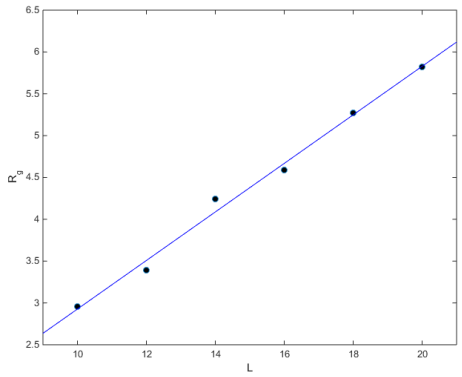

FIG. 4. Radius of gyration R_g of a self-avoiding tethered surface with zero bending rigidity as a function of system size L.

We also plot the R_g as a function of L in Fig. 4 for a self-avoiding tethered surface. The surfaces studied are of limited size. Nevertheless, the relationship appears linear, which supports the absence of a crumpled phase at zero bending rigidity.

Attempts have been made to numerically determine the existence of such a phase by calculating the structure factor,

$$S(\mathbf{k}, L) = \frac{1}{N^2} \sum_{\mathbf{x},\mathbf{x}'} \left\langle e^{i\mathbf{k}\cdot[\mathbf{r}(\mathbf{x})-\mathbf{r}(\mathbf{x}')]} \right\rangle . \tag{15}$$

The structure factor satisfies the scaling form $S(\mathbf{k}, L) = S(kR_g) = S(kL^\nu)$. In [9], the authors found the exponent to be $\nu = 0.83 \pm 0.03$, consistent with the estimate from Flory theory. They conjectured that there exists a crumpling transition in self-avoiding surfaces, but that the details of the transition are different. However, in [15], the authors found the exponent to be $\nu = 0.96 \pm 0.05$, which suggests a flat phase (with $\nu = 1$) even at zero bending rigidity. The data for the above results can be compared in Fig. 5.

It has further been shown by varying the hard-core radius in the excluded volume interaction that self-avoiding tethered membranes are asymptotically flat at zero bending rigidity, and do not undergo a crumpling transition [16].

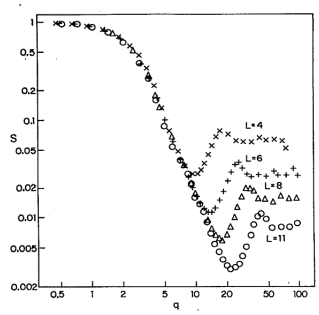

(a)Logarithmic plot of the structure factor S as a function of $q \equiv kL^\nu$ with $\nu = 0.83$ [9].

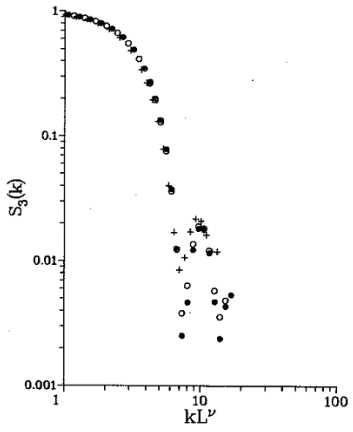

(b)Logarithmic plot of the in-plane structure factor S_3 as a function of kL^ν with $\nu = 0.975$ [15].

FIG. 5. Determination of the scaling exponent ν for self-avoiding tethered surfaces from the structure factor.

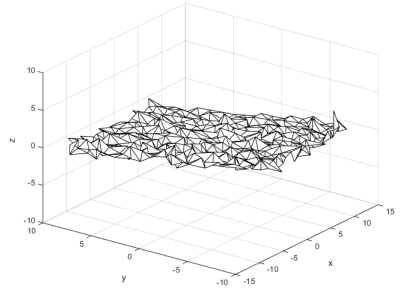

FIG. 6. Monte Carlo simulations for a self-avoiding tethered surface with van der Waals attraction between nearest neighbours.

IV.1. Van der Waals attraction

Finally we consider introducing a van der Waals attraction between nearest neighbours,

$$V_{vdW}(r) = -\frac{U}{r^6}, \quad a < r < b \tag{16}$$

It has been suggested [16] that the self-avoiding constraint introduces an implicit bending rigidity into the surface. It is therefore possible that adding an attractive potential could overcome this bending rigidity and allow for the existence of a crumpled phase. However, in Monte Carlo simulations (see Fig. 6), we do not find a crumpled phase even for a strong van der Waals potential, which suppresses fluctuations that increase the distance between sites.

We note that such simulations approach equilibrium more slowly, because a significantly greater number of

moves are rejected due to the van der Waals potential. It is possible that a crumpled phase exists at equilibrium, but was not reached by the simulated surface.

V. CONCLUSION

The crumpling transition and equilibrium behaviour of tethered surfaces present many interesting features. The phantom surface undergoes a phase transition between a crumpled phase at low bending rigidity and a flat phase at high bending rigidity. The self-avoiding surface, however, does not appear to exhibit such a transition, and is flat even at zero bending rigidity. We also investigate the properties of a self-avoiding surface with nearest neighbour van der Waals attraction. The attractive potential does not induce the surface to crumple. However, due to limitations of the numerical simulations, this result is not conclusive.

In the above discussion, we have restricted ourselves to the study of a single, static surface. There is rich behaviour in the interaction between surfaces as well as the dynamics of the crumpling transition that have not yet been explored as thoroughly.

APPENDIX: MONTE CARLO SIMULATIONS

All Monte Carlo simulations were performed on a triangular lattice with open boundary conditions. The surface was composed of $L \times L$ parallelograms, where L defined the system size. Each simulation began with a perfectly flat surface, and 10^7 iterations were performed. At each iteration, a move is attempted at a random site, and accepted with a probability p determined by the Metropolis algorithm. The move is restricted to a cube with side length δ centered about the original position of the site, with δ chosen such that roughly half of the moves would be accepted.

[1] D. Nelson, T. Piran, and S. Weinberg, *Statistical mechanics of membranes and surfaces*, 2nd ed. (World Scientific Publishing Co. Pte. Ltd., Singapore, 2004).

[2] M. Bowick and A. Travesset, Physics Reports **344**, 255 (1989).

[3] S. Liebler, in *Statistical mechanics of membranes and surfaces*, edited by D. Nelson, T. Piran, and S. Weinberg (World Scientific Publishing Co. Pte. Ltd., Singapore, 2004) 2nd ed., Chap. 3.

[4] S. Liebler, Physics Reports **184**, 265 (1989).

[5] F. David, in *Statistical mechanics of membranes and surfaces*, edited by D. Nelson, T. Piran, and S. Weinberg (World Scientific Publishing Co. Pte. Ltd., Singapore, 2004) 2nd ed., Chap. 7.

[6] A. Košmrlj and D. Nelson, Physical Review E **89**, 022126 (2014).

[7] F. David, Physics Reports **184**, 221 (1989).

[8] D. Nelson and L. Peliti, Journal de Physique **48**, 1085 (1987).

[9] Y. Kantor, M. Kardar, and D. Nelson, Physical Review A **35**, 3056 (1987).

[10] Y. Kantor, in *Statistical mechanics of membranes and surfaces*, edited by D. Nelson, T. Piran, and S. Weinberg (World Scientific Publishing Co. Pte. Ltd., Singapore, 2004) 2nd ed., Chap. 5.

[11] G. Gompper and D. Kroll, in *Statistical mechanics of membranes and surfaces*, edited by D. Nelson, T. Piran, and S. Weinberg (World Scientific Publishing Co. Pte. Ltd., Singapore, 2004) 2nd ed., Chap. 12.

[12] M. Paczuski, M. Kardar, and D. Nelson, Physical Review Letters **60**, 2638 (1988).

[13] L. Landau and E. Lifshitz, *Theory of elasticity*, 3rd ed. (Pergamon Press, 1970).

[14] Y. Kantor and D. Nelson, Physical Review A **36**, 4020 (1987).

[15] M. Plischke and D. Boal, Physical Review A **38**, 4943 (1988).

[16] F. Abraham, W. Rudge, and M. Plischke, Physical Review Letters **62**, 1757 (1989).